LBL--32460

DE92 040379

Amorphous Silicon Pixel Radiation Detectors and Associated Thin Film Transistor Electronics Readout

V. Perez-Mendez, G. Cho, J. Drewery, T. Jing, S.N. Kaplan, A. Mireshghi, D. Wildermuth

Physics Division
Lawrence Berkeley Laboratory
University of California
Berkeley, California 94720

C. Goodman

Air Techniques Corp.
Hicksville, New York 11801

I. Fujieda

NEC Corp.
Kawasaki, Kanagawa, 213, Japan

July 1992

This work was supported by the Director, Office of Energy Research, Office of High Energy and Nuclear Physics, Division of High Energy Physics, of the U.S. Department of Energy under Contract No. DE-AC03-76SF00098.

Amorphous silicon pixel radiation detectors and associated thin film transistor electronics readout

V. Perez-Mendez, G. Cho, J. Drewery, T. Jing, S.N. Kaplan, A. Mireshghi, D. Wildermuth
Lawrence Berkeley Lab, University of California, Berkeley, CA 94720

C. Goodman
Air Techniques Corp., Hicksville, NY 11801

I. Fujieda
NEC Corp., Kawasaki, Kanagawa, 213, Japan

We describe the characteristics of thin (1 μm) and thick (> 30 μm) hydrogenated amorphous silicon p-i-n diodes which are optimized for detecting and recording the spatial distribution of charged particles, x-rays, γ rays and thermal neutrons. For x-ray, γ ray, and charged particle detection we can use thin p-i-n photosensitive diode arrays coupled to evaporated layers of suitable scintillators. For thermal neutron detection we use thin (2~5 μm) gadolinium converters on 30 μm thick a-Si:H diodes. For direct detection of minimum ionizing particles and others with high resistance to radiation damage, we use the thick p-i-n diode arrays. Diode and amorphous silicon readouts as well as polysilicon pixel amplifiers are described.

1. INTRODUCTION

Thin layers of hydrogenated amorphous silicon (a-Si:H) with thickness 0.5 - 1 μm have found extensive application in solar cells and in thin film transistors (TFT). A well known application of thick > 30 μm layers of a-Si:H is to electrophotography devices. In all these devices the usual configuration is that of a p-i-n diode with very thin (50 nm) p^+ and n^+ doped layers and the bulk consisting of intrinsic a-Si:H. For radiation detection we use the same general configuration of a reverse biased p-i-n diode. In many of the applications that are useful in physics, the spatial distribution of the incident radiation is important: hence we use pixel or strip configurations with appropriately shaped metallic contacts. In some applications single particles are detected; the detector array then requires individual, low noise TFT amplifiers attached to each pixel. Other applications are to radiation flux detection: for these, simple routing electronics may be sufficient. These configurations of detector and TFT arrays are shown schematically in Fig. 1. Charged particle detection - specifically minimum ionizing particles (MIPs) can be accomplished by use of p-i-n diodes with thick i-layers in which the charged particle can produce a sufficient number of electron-hole pairs by direct interaction in the depleted i-layer. An alternative scheme for MIPs detection is to use pixel/strip arrays of thin a-Si:H diode layers - which function as visible photon sensors - coupled to layers of light emitting (scintillator) material, such as cesium iodide. For the detection of x-rays or γ rays of energy above a few KeV, the scintillator - a-Si:H array is the only feasible choice due to the low interaction probability of the radiation with a low Z element such as silicon. For detection of x-rays in x-ray crystallography applications (Eγ = 8 KeV), it is also possible to use

This work was supported by the U.S. Department of Energy under contract #DE-AC03-76SF00098.

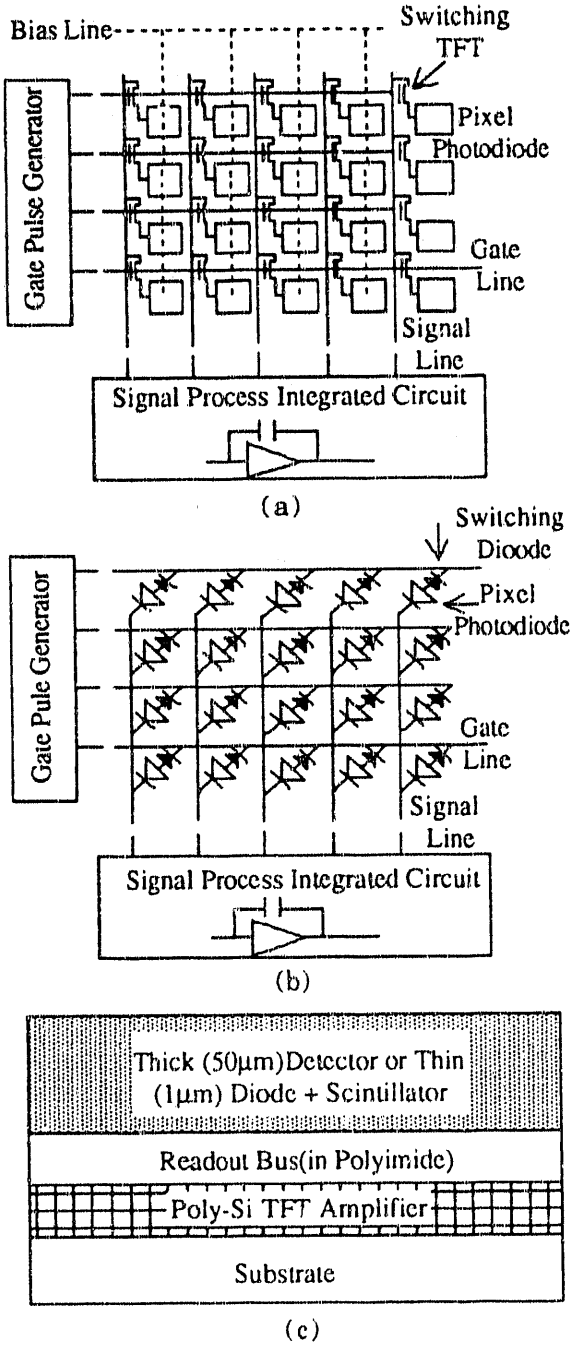

Fig. 1. Readout electronics arrays (a) TFT readout (b) diode readout (c) structure for amplifier/pixel readout.

moderately thick layers of a-Si:H (80%) + a-Ge:H (20%) where the germanium is the high Z element, contributing to the interaction.

The potential usefulness of amor-phous silicon as a detector material is due to the following (a) It is readily made by inexpensive plasma enhanced chemical vapor deposition (PECVD) techniques in large areas > 30 x 30 cm: (b) it is very radiation resistant to fast neutrons, charged particles and γ rays: (c) dispersed thin film transistor (TFT) electronics for reading out pixel or strip arrays is readily made by the same PECVD technologies in an integral manner.

2. DETECTION OF CHARGED PARTICLES WITH THICK P-I-N DIODES

A reverse biased diode with a thick i-layer requires use of a-Si:H with a low density of dangling bonds (< 2 x 10^{15}/cm^3) for the following reasons: (a) The mean free path of electrons and holes is $d = \mu\tau E$ where μ, τ, are the mobilities and lifetimes of the electrons or holes and E = the electric field of the external bias; therefore a large value of $\mu\tau$ is desirable since $\mu\tau N_d \approx 2.5 \times 10^8$.[1] (b) When an external bias is applied, a fraction of the neutral dangling bonds $N_d^* \approx 0.3\ N_d$.[2] are ionized and a residual positive charge remains. This fixed, positive charge causes the electric field in the i-layer to drop linearly with distance, until a low electric field < 5 x 10^4 V/cm is reached at which point the E field decreases exponentially.[3] Hence, in order to have a fully depleted detector, a minimum bias is needed which increases proportionately to the density of dangling bonds. The electric field peaks at the p-i interface which is close to the metal contact and at high biases enhances breakdown. The following schemes to promote full depletion without breakdown have been developed [4, 5] as shown in Fig. 2.(a) The p-layer is made considerably thicker, i.e., 200 - 400 nm which places the

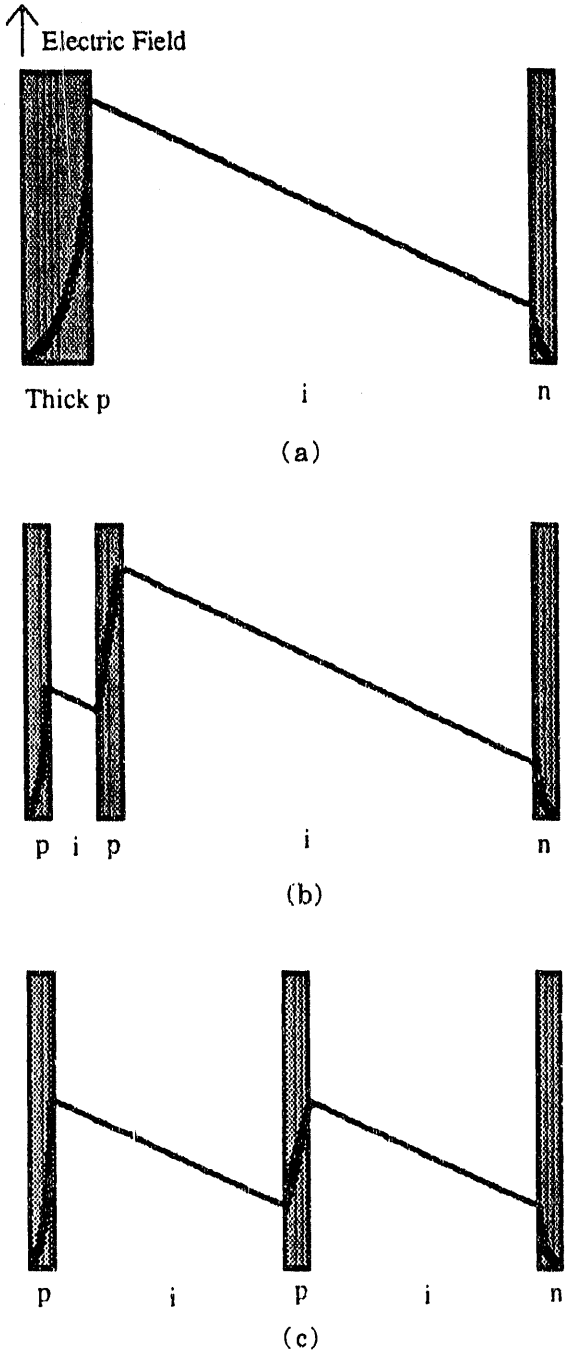

Fig. 2. Field shaping configurations (a) thick p-layer (b) buried p-layer adjacent to contact (c) buried p-layer in the center of i-layer.

peak E field further away from the metal contact. (b) A buried, thin ~20 nm thick p-layer is deposited with a ~1 μm spacing to the electrode. Schemes (a) and (b) increase the allowable bias potential by ~3 times. (c) One or more thin p-layers are deposited in the middle of the i-layer whose effect is to decrease the effective slope of the electric field since the p-layer, under bias, leaves a residual negative charge. With one p-layer of the appropriate thickness, the applied bias for full depletion can be lowered by ~2.[6] Schemes (a) and (b) cause little or no loss in the number of charged carriers traversing the i-layer. Scheme (c) causes some electron loss due to trapping because of the lower mean free path in the p-layer, whereas the hole loss is minimal.[7] An important quantity in evaluating the interaction of charged particles with an a-Si:H p-i-n diode is W = average energy used in producing 1 e-h pair. We measured W using an 860 MeV alpha particle beam - essentially MIPs [3] and found W = 4.8 ± 0.3 eV. This corresponds to a production rate by MIPs of ~80 e-h pairs/μm of a-Si:H.

The noise produced in a reverse biased p-i-n detector together with that of a typical readout amplifier should be small. In Fig. 3 we show the noise in a 26 μm diode as a function of reverse bias, measured by a charge sensitive amplifier with 2.5 and 0.5 μsec CR-$(RC)^2$ shaping times. The flat portion of the noise graph, at low biases, is the sum of (a) the amplifier noise when loaded by the capacity of the detector, and a mostly resistive (Nyquist) noise generated by the contact and the p-layer resistance. The noise contribution of the p-layer resistance can be reduced by annealing (~2 hours at 180 °C) under bias.[8] At higher biases when the reverse current increases, the contributing shot noise - which has a flat frequency spectrum and is proportional to the current is observed. At still higher biases with larger reverse current, 1/f noise, which has the 1/f spectral response and is proportional to the

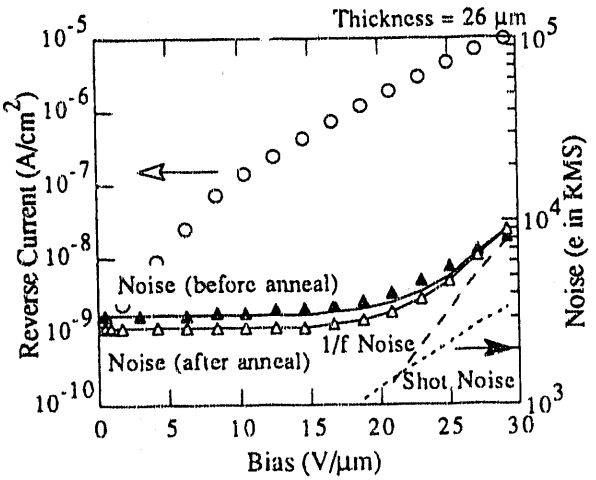

(a)

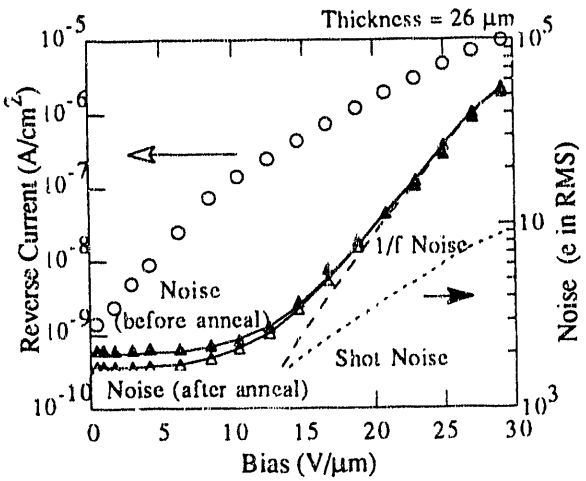

(b)

Fig. 3. Reverse current and noise for 26 μm thick p-i-n diode (a) 2.5 μsec shaping time (b) 0.5 μsec shaping time.

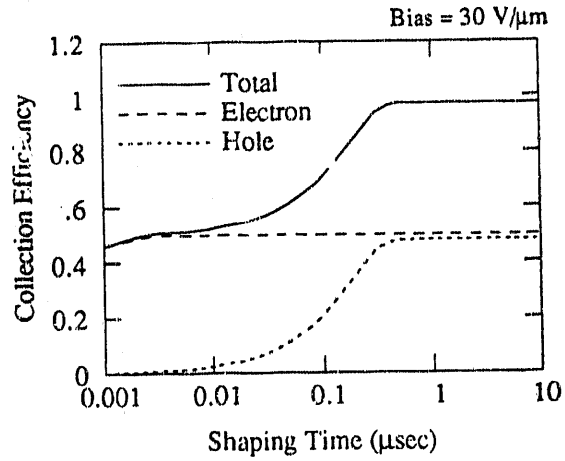

(a)

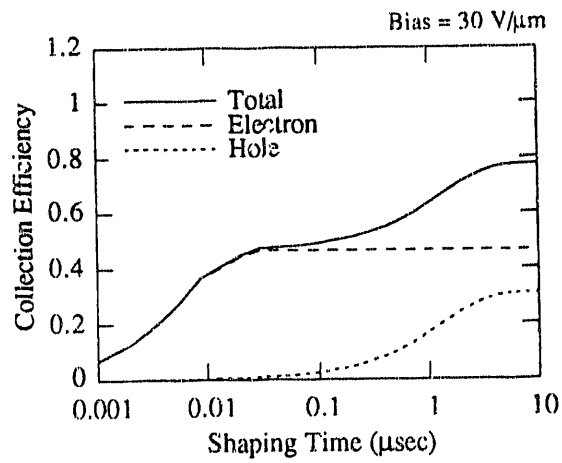

(b)

Fig. 4. Normalized electron and hole collection efficiency (a) 1 μm thick diode (b) 50 μm thick diode.

current squared, becomes the predominant contribution. All of these noise compo-nents are proportional to the area of a pixel detector. The signal response as a function of shaping time can be calculated from the mobility - typically μ_e ~ 1 cm^2/Vsec, μ_h ~ 0.005 cm^2/Vsec, and the E field in the i-layer at a given bias. Fig. 4 shows the signal from electrons and holes for thin (1 μm) and thick (50 μm) detector diodes. Fast timing for both is achieved by collecting the full electron signal only in < 5, 20 nsec respectively. We measured the radiation damage produced by fast (1 MeV) neutrons on various p-i-n diodes and found that the reverse currents, signal and noise changed by less than 10 % up to neutron fluxes of 5 x 10^{14} N/cm^2.[9]

3. DETECTION OF RADIATION BY THIN A-SI:H DIODES COUPLED TO SCINTILLATOR LAYERS

For this case we assume that the signal is produced predominantly by the interaction of the radiation with the scintillator and that the scintillation light is then detected by the a-Si:H through a transparent, conducting,

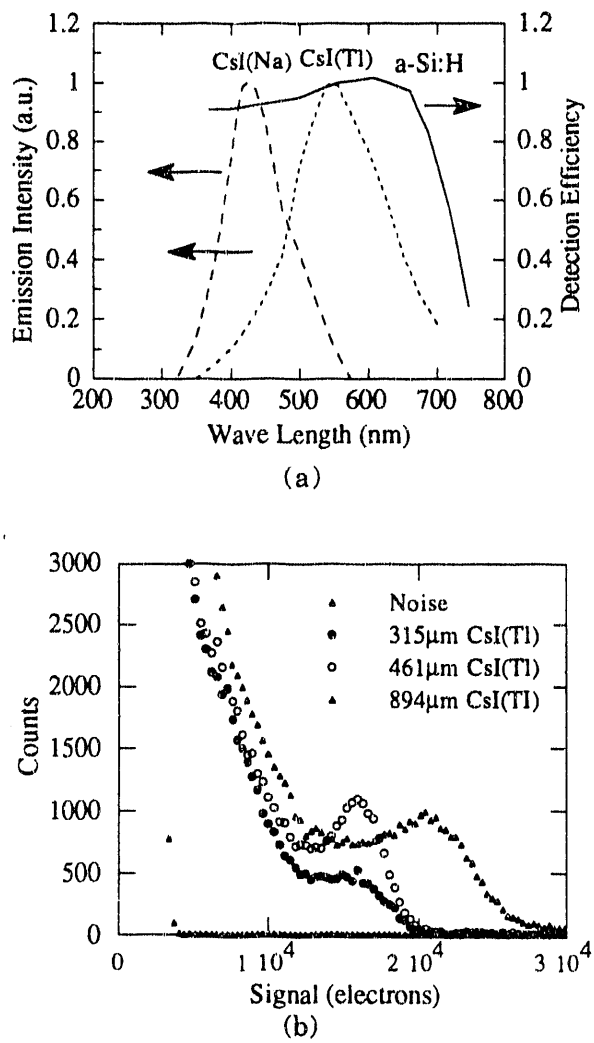

Fig. 5. CsI/a-Si:H detectors (a) emission spectra of CsI(Tl), CsI(Na) and a-Si:H response (b) signal from 1 MeV betas for various CsI(Tl) thickness.

indium tin oxide contact. A further requirement - if good position accuracy in a pixel or strip detector is desired - is that the scintillation light be suitably collimated. We have worked primarily with evaporated layers of CsI activated with thallium. The CsI(Tl) has been measured [10] to produce > 50,000 visible light photons/MeV of absorbed radiation energy - charged particles, x-rays or γ rays. The spectral emission of CsI(Tl), shown in Fig. 5a, is in the λ = 400 - 700 μm range for which a 1μm thick a-Si:H diode has a flat response. For the CsI(Tl), the light to e-h pairs in a-Si:H conversion is > 70%. We measured that the signal size in a CsI(Tl)/a-Si:H combination is ~40,000 e-h pairs per MeV of energy deposited in the CsI layer. Fig. 5b shows the response of 1 MeV betas from a Bi-209 source for various CsI/Silicon detector combinations.

Some light collimation is achieved by inducing some structure to develop through the CsI(Tl) layer by controlling the cooling rate of the substrate in the evaporation process.[11, 12] We have obtained better light collimation - hence better spatial resolution by evaporating CsI(Tl) on to etched patterned substrates of polyimide (Fig. 6a,b) [13] deposited on the a-Si:H surface or on a glass or metal substrate. The point spread function produced by an x-ray beam incident through a 25 μm aperture and measured by a linear detector array is shown in Fig. 6b. The better columnar structure produced by the patterned substrate compared to the thermally induced pattern produces point spread functions which are ~2.5 narrower than those from the plain substrate. Another quantity of interest is the resistance of the device to radiation. As noted previously, the a-Si:H diodes and TFT are very radiation resistant. CsI(Tl) crystals are considerably more susceptible to radiation damage. In general it has been shown that the main loss in crystal scintillators is due to decrease of light transmission through the bulk of a crystal. We confirmed this by measuring the signal decrease for a 1 cm^3

(a)

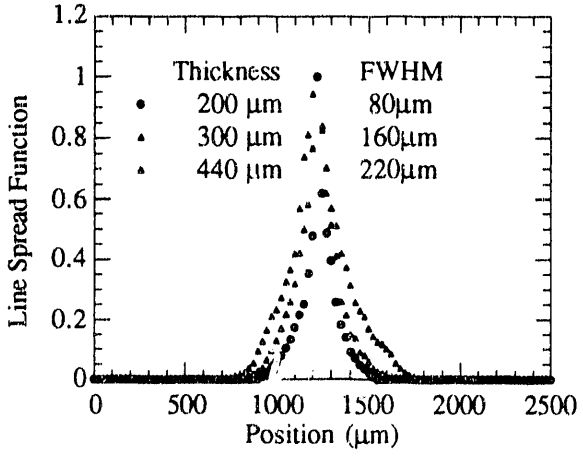

(b)

Fig. 6. (a) Columnar structure produced by 30 μm circular polyimide pattern (b) Spatial resolution produced by rectangular polyimide pattern with 40 μm pitch.

CsI(Tl) crystal and an evaporated layer 200 μm thick and we show that the thin layer has a radiation resistance ~100 higher than the crystal.[14] The measured signal [14] produced by electrons (MIPs) from a Sr-92 beta source; as shown in Fig. 5b signal is > 15,000 e-h pairs; this is more than sufficient for the detection of individual particles in a pixel/strip array with simple, low noise, TFT or diode routing electronics.

4. PIXEL ARRAY DETECTION OF THERMAL NEUTRONS

Thermal neutron detection with position sensitivity is useful for neutron radiography and for neutron crystallography in locating the position of hydrogen atoms in the crystal lattice. Thermal neutrons can be detected in pixel arrays by use of gadolinium converters plated on to the metallic contacts of 30 μm thick a-Si:H diodes. Natural gadolinium contains various isotopes whose cross section for thermal neutron capture is 46,000 barns followed by the emission of an 80 keV electron internal conversion line. A 30 μm thick a-Si:H diode can absorb the full energy of these electrons yielding a signal of ~12000 electron-hole pairs. Monte Carlo calculations and experimental measurements show that a 2 μm thick gadolinium layer in such a combination yields a detection efficiency of ~25%.[15] Background from γ rays is negligible in such a detector, due to the low interaction in the gadolinium and the a-Si:H. Further calculation shows that if we use the enriched isotope Gd-157 with a thermal neutron capture cross section of ~250,000 barns we can achieve a detection efficiency of > 80%.

5. THIN FILM TRANSISTOR (TFT) READOUTS FOR PIXEL ARRAYS

In Fig. 1 we showed schematically TFT and diode methods for reading out a-Si:H pixel detector arrays. The structure of a-Si:H and of polysilicon TFT are shown in Fig.

7a,b. Notice that the dielectric layer is silicon nitride for the amorphous silicon TFT and silicon dioxide for the polysilicon TFT. The diode readout configuration - which requires a lesser number of lithographic masks for production is shown schematically in Fig. 7c. The SVX chip, which is a 128 input low noise amplifier that we use for this kind of matrix readout is described in Ref. 16.

Properties of typical a-Si:H and polysilicon TFT are given in Table I below and in Fig. 8.

Table I. Typical properties of a-Si:H and polysilicon TFTs

Type	a-Si:H TFT	poly-Si TFT
μe (cm^2/Vsec)	1	150
μh (cm^2/Vsec)	.005	80
gm (μA/V)	5	150
Bandwidth(MHz)	5	100
Noise*(e)	500	500

* Equivalent noise charges for an CR-$(RC)^4$ shaping time of 1 μsec.

Amorphous silicon TFT can only be used as switching devices because the threshold voltage of the gate bias shifts continuously under dc bias.[17] True CMOS amplifiers can be made using polysilicon TFT since both electron and hole mobilities are comparable and much higher than the corresponding ones for a-Si:H TFT as shown in Table I.

In Fig. 8a we show typical drain-source current curves for one NMOS polysilicon transistor with gate width L = 5 μm and length W = 50 μm. We measured the characteristics of various polysilicon TFT with similar dimensions. A typical noise versus frequency curve is shown in Fig. 8b. The predominant noise component is 1/f noise and that can be minimized by using short shaping times.[18]

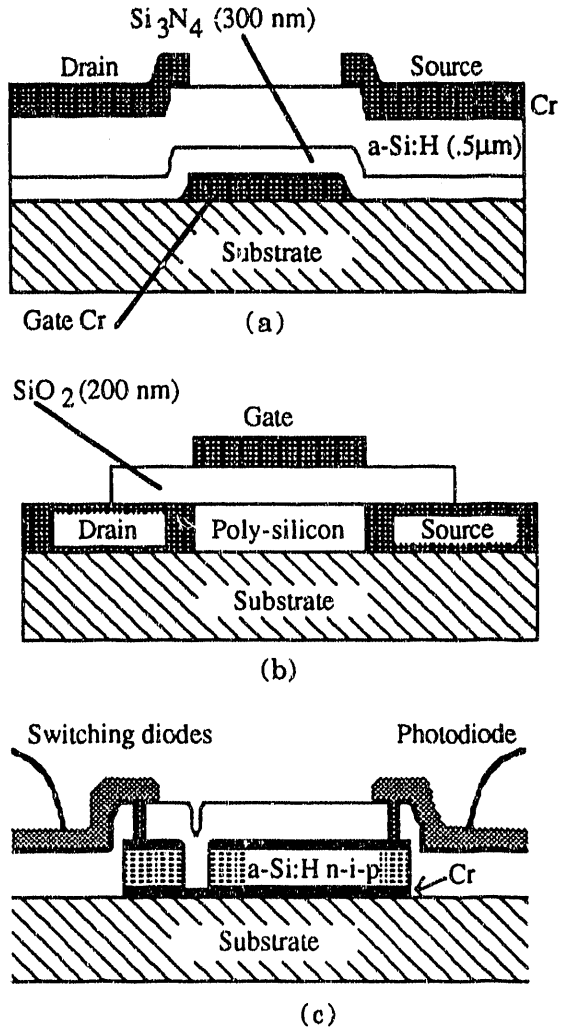

Fig. 7. Structure of TFTs and diode readout (a) a-Si:H TFT (b) polysilicon TFT (c) diode readout cross section.

Using the facilities of the Xerox research lab in Palo Alto, we designed and tested 3 stage CMOS polysilicon amplifiers with a charge sensitive input stage followed by a voltage gain stage, followed by a low impedance output stage for driving signals through a pixel array. This prototype amplifier design is shown in Fig. 9. The measured characteristics are given below in Table II.

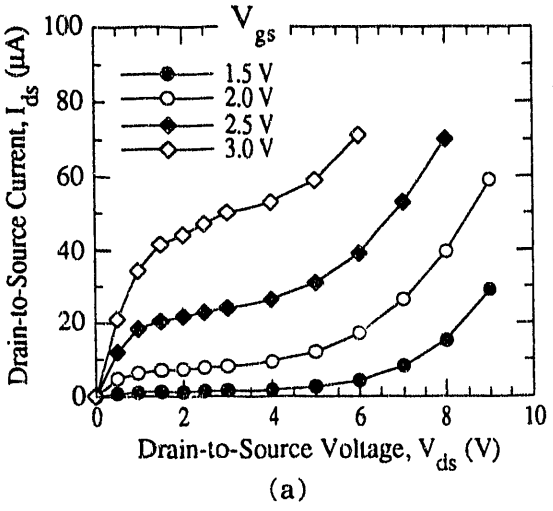

(a)

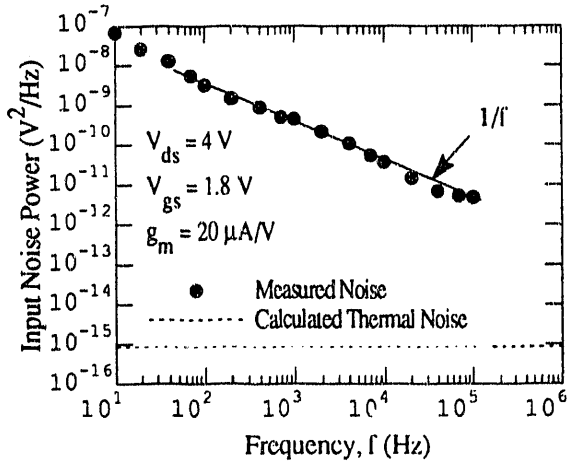

(b)

Fig. 8. Characteristics of polysilicon TFTs (a) drain-source current versus gate voltage (b) measured noise.

Table II. Characteristics of polysilicon TFT charge-sensitive amplifier

Dimension	< 200 x 200 μm^2
Charge gain	~ 0.02 mV/electron
Rise time	100 nsec
Bandwidth	3.5 MHz
Noise	~ 1000 electrons
Power dissipation	< 1 mW/pixel

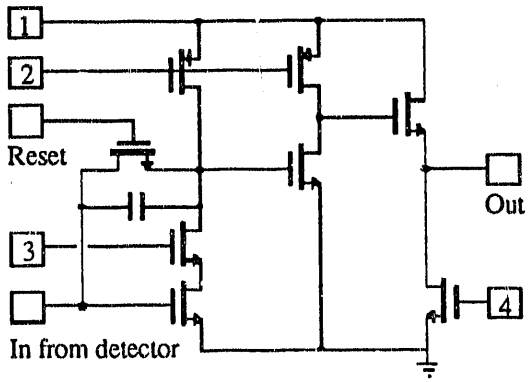

Fig. 9. Schematic polysilicon CMOS charge-sensitive amplifier. (Nodes are an input, an output, a reset and 4 bias-nodes.)

6. SUMMARY AND CONCLUSIONS

At present the technology which is ready for use is the thin photosensitive p-i-n diode array coupled to an evaporated layer of CsI(Tl) deposited on a patterned substrate to produce good spatial resolution. Furthermore, the larger signals obtained from MIPs from this combination compared to those from a 50 μm direct interaction p-i-n diode simplify the electronic array necessary for readout of both flux distributions and single particles. The main disadvantage of this configuration is that it is less radiation hard than the monolithic a-Si:H detector. At present, the main difficulty with the thick a-Si:H diodes is that they are produced with a large compressive stress.

ACKNOWLEDGEMENTS

We acknowledge the contribution of R. Hollingsworth, J. Xi from the Materials Research Group (formerly Glasstech-Solar, Wheat Ridge, Co.) for making the p-i-n detectors. We also thank M. Hack, A. Lewis and I-Wei Wu from Xerox Parc for their help in the design and fabrication of TFT electronics. We also thank G. Weckler from EG&G Reticon for the use of various linear readout diode arrays.

REFERENCES:

1. R. A. Street, Phys. Rev. B 27 (1983) 4294.
2. S. Qureshi, V. Perez-Mendez, S. N. Kaplan, I. Fujieda, G. Cho, R. A. Street, Mat. Res. Symp. 149 (1989) 649-654.
3. V. Perez-Mendez, Chapter 8 in "Physics and Applications of Amorphous and Microcrystalline Semiconductor Devices", J. Kanicki, Ed., Artech House Pub., Boston, MA (May 1991).
4. I. Fujieda, G. Cho, J. Drewery, S. N. Kaplan, V. Perez-Mendez, S. Qureshi, D. Wildermuth, R. A. Street, Mat. Res. Symp. 192 (1990) 399-404.
5. T. Pochet, J. Dubeau, L. A. Hamel, B. Equer, A. Karar, Mat. Res. Soc. 149 (1989) 661. Also B. Equer Mat. Res. Soc. 258 (to be published).
6. J. Drewery, G. Cho, T. Jing, S. Kaplan, A. Mireshghi, V. Perez-Mendez, D. Wildermuth, to be published Mat. Res. Soc. 258 (Oct 1992).
7. R. A. Street, J. Zesch, M. J. Thompson, App. Phys. Letters 43 (193) 672-676.
8. S. Qureshi, G. Cho, J. Drewery, T. Jing, S. N. Kaplan, A. Mireshghi, V. Perez-Mendez, D. Wildermuth, R. A. Street, to be published in IEEE Trans. Nuc. Sci. NS 39 (1992).
9. V. Perez-Mendez, S.N. Kaplan, G. Cho, I. Fujieda, S. Qureshi, W. Ward and R.A. Street, Nuc. Instr. and Methods, A273 (1988) 127-134.
10. L. Holl, E. Lorenz, G. Mageras, IEEE Trans. Nuc. Sci NS 35 (1988) 105-109.
11. C. W. Bates, Adv. Electronics and Electron Physics 28A (1968) 451-459.
12. A.L.N. Stevels and A.D.M. Schrama de Pauw, Phillips Res. Rpts. 29 (1974) 340-362.
13. DuPont Photosensitive Polyimide Resin Pyralin PD PI 2722.
14. I. Fujieda, G. Cho, J. Drewery, T. Gee, T. Jing, S. N. Kaplan, V. Perez-Mendez, D. Wildermuth, R. A. Street, IEEE Trans. Nuc. Sci. NS 38 (1991) 255-262.
15. A. Mireshghi, G. Cho, J. Drewery, T. Jing, S. N. Kaplan, V. Perez-Mendez and D. Wildermuth, To be published in IEEE Trans. Nuc. Sci., NS-39 (1992).
16. S. A. Kleinfelder, W. C. Carithers, R. P. Ely, C. Haber, F. Kirsten, H. Spieler, IEEE Trans. Nuc. Sci. NS-35 (1988) 171.
17. W.B. Jackson and M.D. Moyer, Phys. Rev., B36, 6217 (1987)
18. G. Cho, V. Perez-Mendez, M. Hack and A. Lewis, LBL-32219 (April 1992). To be published in Mat. Res. Soc 258 (Oct 1992).

END

DATE
FILMED
10/30/92